Open access • Journal Article • DOI:10.1158/0008-5472.CAN-19-3230

Targeting p63 Upregulation Abrogates Resistance to MAPK Inhibitors in Melanoma.

Ankit Kumar Patel, Lucia Fraile Garcia, Viviana Mannella, Luke Gammon ...+12 more authors

Institutions: Queen Mary University of London, University of Milan, Technische Universität München, Sigmund Freud University Vienna ...+1 more institutions

Published on: 15 Jun 2020 - Cancer Research (American Association for Cancer Research (AACR))

Topics: Downregulation and upregulation, MAPK/ERK pathway, Melanoma and Mdm2

Targeting p63 upregulation abrogates resistance to MAPK inhibitors in melanoma

Ankit Patel[1], Lucia Fraile Garcia[1], Viviana Mannella[1], Luke Gammon[1], Tiffanie-Marie Borg[1], Tania Maffucci[1], Maria Scatolini[2], Giovanna Chiorino[3], Elisabetta Vergani[4], Monica Rodolfo[4], Andrea Maurichi[5], Christian Posch[6,7,8], Rubeta N. Matin[9], Catherine A. Harwood[1] & Daniele Bergamaschi[1]*

[1] Centre for Cell Biology and Cutaneous Research, Blizard Institute, Barts and The London School of Medicine and Dentistry, Queen Mary London University, London E1 2AT, UK.

[2] Molecular Oncology Lab, Fondazione Edo ed Elvo Tempia, 13900 Biella (Italy)

[3] Cancer Genomics Lab, Fondazione Edo ed Elvo Tempia, 13900 Biella, Italy.

[4] Department of Experimental Oncology and Molecular Medicine, Immunotherapy Unit, Fondazione IRCCS Istituto Nazionale Tumori, 20133 Milan, Italy.

[5] Department of Surgery, Melanoma and Sarcoma Unit, Fondazione IRCCS Istituto Nazionale Tumori, 20133 Milan, Italy.

[6] The Rudolfstiftung Hospital, Department of Dermatology, Vienna, Austria,

[7] Sigmund Freud University, Faculty of Medicine, Vienna, Austria,

[8] Technical University of Munich, Department of Dermatology, Munich, Germany.

[9] Department of Dermatology, Oxford University Hospitals NHS Foundation Trust, Headington, Oxford, OX3 7LE, U.K.

* Corresponding author:

Tel.	44207882 2567
FAX.	44207882 7172
e-mail:	d.bergamaschi@qmul.ac.uk

Running Title: *p63 impact in MAPK inhibitors resistant melanoma*

Key words: BRAF, melanoma, TP63, FBXW7, MDM2, MAPK inhibitors-resistance

Conflicts of interest: The authors declare no potential conflicts of interest.

Word counts: 5550

N. of figures: 6 figures + 1 Table + 5 Supplementary figures

ABSTRACT

Targeting the MAPK pathway by combined inhibition of BRAF and MEK has increased overall survival in advanced BRAF-mutant melanoma in both therapeutic and adjuvant clinical settings. However, a significant proportion of tumors develop acquired resistance, leading to treatment failure. We have previously shown p63 to be an important inhibitor of p53-induced apoptosis in melanoma following genotoxic drug exposure. Here we investigated the role of p63 in acquired resistance to MAPK inhibition and show that p63 isoforms are upregulated in melanoma cell lines chronically exposed to BRAF and MEK inhibition, with consequent increased resistance to apoptosis. This p63 upregulation was the result of its reduced degradation by the E3 ubiquitin ligase FBXW7. FBXW7 was itself regulated by MDM2, and in therapy-resistant melanoma cell lines, nuclear accumulation of MDM2 caused downregulation of FBXW7 and consequent upregulation of p63. Consistent with this, both FBXW7 inactivating mutations and MDM2 upregulation were found in melanoma clinical samples. Treatment of MAPK inhibitor-resistant melanoma cells with MDM2 inhibitor Nutlin-3A restored FBXW7 expression and p63 degradation in a dose-dependent manner and sensitized these cells to apoptosis. Collectively, these data provide a compelling rationale for future investigation of nutlin-3A as an approach to abrogate acquired resistance of melanoma to MAPK inhibitor targeted therapy.

SIGNIFICANCE

Upregulation of p63, an unreported mechanism of MAPK inhibitor resistance in melanoma, can be abrogated by treatment with the MDM2 inhibitor Nutlin-3A, which may serve as a strategy to overcome resistance.

INTRODUCTION

Advanced melanoma is an aggressive cancer. Discovery of the oncogenic mutation BRAFV600E led to development of targeted BRAF inhibitors, which have significantly prolonged overall survival and progression-free in advanced melanoma (1). Combined BRAF and MEK targeted therapy increases the rate and durability of treatment responses and this combination therapy is now used in both therapeutic and adjuvant clinical settings (2). However, despite initially impressive clinical responses, most patients with advanced melanoma treated with MAPK inhibitors develop acquired resistance within 6 to 7 months (3). Resistance is an important clinical challenge and understanding the mechanisms of resistance is currently an area of intense research activity.

TP63 is critical for the development and maintenance of squamous epithelia. It is mainly expressed in the basal layers of stratified epithelial tissues where is considered a cell lineage specific marker (4). TP63 has been linked to chemosensitivity in a number of tumours and is a biomarker for poor prognosis in breast cancer and follicular cell lymphoma (5) (6). We previously provided the first evidence supporting an oncogenic role for p63 in melanoma. We reported up-regulation of p63 mRNA and protein in melanoma and induction of p63 nuclear stabilization and partial relocation to the mitochondria in response to DNA-damaging agents. Consequently, p63 has an anti-apoptotic role in melanoma, contributing to chemoresistance and its expression correlates with melanoma-specific death (7).

Multiple ligases degrade p63 in keratinocytes. This include E3 ubiquitin ligases (Nedd4, Itch and its homologue WWP1) and Ubc9, a SUMO-conjugating enzyme. Pirh2 (p53-induced RING-H2) also modulates keratinocyte differentiation by targeting both TA and ΔNp63 for proteasomal degradation (8-16).

FBXW7 is a E3 ubiquitin ligase which contributes to p63 degradation in keratinocytes (17) and functions as a potent tumour suppressor with many oncoprotein targets. FBXW7 is also mutated in about 8% of melanomas and is inactivated in about 40% of melanoma cell lines

(18). In keratinocytes, MDM2 and FBXW7 cooperatively control the stability of p63 protein during keratinocyte differentiation and UV irradiation. MDM2 binds with ΔNp63 and transports it into the cytoplasm where its phosphodegron domain is recognized by FBXW7 (17). HDAC inhibitors (HDACi) reduce ΔNp63 protein levels via FBXW7 E3 ubiquitin ligase (19).FBXW7 is alternatively spliced to produce three C-terminal isoforms, alpha, beta and gamma (20-24). The cellular localization signal is in the C-terminal variable region, while the N-terminal region includes seven WD40 domain, which recognizes and binds with its target protein, and is conserved between different isoforms. Several inactivating mutations are reported in this WD40 region, which selectively loses the capacity to target specific protein in human tumours (25-28).

MDM2 and MDM4 are potent oncogenes and are commonly over-expressed in cancer, including melanoma. They are well-known inhibitors of p53 and in normal tissues maintain p53 at reduced intracellular levels by mediating its rapid degradation and subsequently inhibiting its transcriptional activity (29-32). P53 mutations are common in many UV-associated skin cancers (33), but are less common in melanoma, present in up to 19% as a point mutation, and in the remaining wild type (wt) tumours, p53 is often inactivated by other mechanisms (34), such as MDM2 amplification.

MDM2 and MDM4 amplification, although mutually exclusive, are often involved in mechanisms of wild type p53 inactivation in melanoma (35-38) and targeting MDM2 is a recognised therapeutic approach in wt TP53 cancers. Nutlin-3A, a small molecule MDM2 inhibitor, prevents its association with p53 leading to wt p53 accumulation and reactivation (39). Nutlin-3A also stabilizes p73 and stimulates p53 independent pro-apoptotic activities (40). Nutlin-3A is currently used as an anti-tumour agent both in vitro and in vivo, targeting solid tumours including melanoma, breast cancer, prostate cancer, retinoblastoma and haematological malignancies (41). Nutlin-3A treatment downregulates IGF-1R protein levels by stabilizing MDM2 and increases migratory capacity of melanoma cells via ERK activation,

although reduces their invasive potential by destabilizing MAPK/PI3K balanced activation leading to disrupted IGF-1R - MMP2 activation (42).

Here we investigate a possible role for p63 involvement in acquired resistance to MAPK inhibition, characterising p63 expression and mechanisms of p63 regulation upon acquisition of MAPK inhibitor resistance. We also provide a rationale for the use of Nutlin-3A as an approach to reducing acquired resistance associated with therapeutic MAPK inhibition in melanoma.

MATERIAL AND METHODS

Cell culture. HaCaT, HCT116 and HEK293T cells were cultured in DMEM medium supplemented with 10% FCS and 1% pen/strep antibiotic solution. All melanoma cell lines were cultured in RPMI-1640 medium supplemented with 10% foetal calf serum (FCS) and in antibiotic free conditions. Establishment of vemurafenib or Trametinib resistant melanoma cells was performed on BRAFV600E mutated cell lines seeded and treated with increasing doses of PLX4032 or Trametinib for at least 1 month. Media with fresh drug was replaced every other day and cells were split when necessary. Afterwards PLX4032 drug dose was maintained to 3μM and Trametinib for 50nM. Cells were used in further experiments only after the resistance was confirmed. Cell lines LM16, LM17 and LM36 (sensitive and PLX-resistant) kindly provided by Dr Monica Rodolfo, where established in another laboratory following similar procedure.

Protein extraction and western blotting. Equal amount of protein lysates was resuspended in 10X NuPage reducing agent (500mM DTT, Invitrogen #NP0009) and 4X NuPage Lithium dodecyl sulphate (LDS) sample buffer (Invitrogen # NP0007). Samples were mixed and heated at 70°C for 10 minutes. Protein samples were resolved using 10% Bis-Tris gels. The fast transfer was performed using the BioRad Trans-Blot® Turbo™ RTA Mini PVDF Transfer Kit (#1704274) with Trans-Blot® Turbo™ system at 25A and 2.5V for 10 minutes. Upon completion of protein transfer, the membrane was washed with dH_2O and left for blocking for 1 hour with 5% BSA (Sigma). The membrane was incubated with primary antibody at +4°C for

overnight. The next day, after 3 x 10 minutes PBS Tween-20 0.1% (PBST) washings, the membrane was incubated with anti-mouse antibody (DAKO) diluted 1:5000 (vol/vol) or anti-rabbit antibody (DAKO) diluted 1:10000 (vol/vol) in PBST supplemented with 1% BSA for 1 hour at room temperature. The membranes were washed three times with PBS-Tween 0.1%, and bound secondary antibody was detected by enhanced chemiluminescence with ECL Plus (GE Healthcare) according to the manufacturer's protocol. For cytoplasmic and nuclear protein extraction, cells pellet was resuspended in 300µl hypotonic buffer. Later mixed with 25µl 10% NP40 (detergent) reagent and vortexed for 20 seconds followed by 10 minutes centrifugation at 3000 rpm at 4ºC. Then carefully supernatant was collected in separate tube labelled as cytoplasmic fraction. The nuclear pellet was gently washed twice with ice-cold PBS to avoid the contamination from cytoplasmic fraction. Nuclear pellet was resuspended in 50µl complete Cell Extraction buffer (#FNN0011, Thermo-Fisher) followed by 30 minutes incubation on ice with vortexing at every 10 minutes intervals. The cells debris was removed by 30 minutes centrifugation at full speed at 4ºC. The supernatant (nuclear fraction) was collected into a clean microcentrifuge tube. These both fractions were analysed on SDS-PAGE as previously described. Antibodies used: p63 (#SFI-6, DSC Diagnostics Germany), p63 (#M731729-2, Dako, Agilent Technologies LDA UK Limited) p63 (#H137, Santa Cruz), GAPDH (Generon), MDM2 (#N20, Santa Cruz), FBXW7 (#109617, abcam).

In vitro ubiquitination assay. In vitro ubiquitination assay performed with Abcam (ab139469) kit using purified recombinant FBXW7 protein. As per the kit protocol, two control reactions (without ATP or MDM2) and final reactions with recombinant FBXW7 mixed together. The reactions were incubated at 37°C for 90 minutes and terminated with 2x SDS-PAGE gel loading buffer followed by heating at 95°C. The reaction products were subsequently analysed by SDS-PAGE and chemiluminescent western blot.

shRNA. Genes were stably silence using pLKO.Puro lentiviral system. For p63: GAAGAAACTCTACTGCCAAAT, GAATTCAACGAGGGACAGATT and for FBXW7: GCAACAACGACGCCGAATTAC, GGACTCCTCAGGAAACCAAGA and scramble:

TGTTATACGATTTCCTGCACC sequences were cloned in pLKO.Puro vector according to Addgene protocol. pLenti-puro was a gift from Ie-Ming Shih (Addgene plasmid # 39481).

DNA mutation analysis. Paraffin embedded tissues derived from each lesion were macro-dissected and DNA was isolated by using QIAamp DNA micro Kit (Qiagen). BRAF exon 15 and NRAS exons 2 and 3 were amplified by previously optimized PCR primers and conditions. PCR products were purified by ExoSAP-IT (USB Corporation, Cleveland, Ohio) and sequenced using Big Dye Terminator V3.1 Cycle Sequencing Kit on AB3500dx DNA Analyzer (Life Technologies). Sequence analysis was performed by Variant Reporter (Life Technologies).

Immunohistochemistry. Paraffin embedded tissue samples material representing different stages of melanoma development analysed in this study were obtained from Barts and the London NHS Trust. The investigators obtained informed written consent from the patients. All patients' data collected and used in the manuscript has been consented with an institutional review board-approved protocol that allows comprehensive analysis of tumour samples and covered by an ethical approval [07/QO604/23 by the East London & The City HA Local Research Ethics committee 2, UK]. Tissue samples were fixed in 10% formal saline solution before being embedded in paraffin wax. 3-4 µm sections were mounted onto a positively charged slide, dewaxed in xylene twice for 3 min and rehydrated in alcohol twice for 3 min before being placed in running water for 5 min. Antigen retrieval for p63 staining, slides were microwaved in Tris-EDTA unmasking solution pH9 for 35 min. Following antigen retrieval sections were placed in running water for 5 min before endogenous peroxidase activity was blocked by incubation with 3% hydrogen peroxide solution for 15 min. Sections were washed three times in wash buffer before Normal Horse Serum (Vector R.T.U. kit, Vector Labs) was applied for 20 min. The serum was then replaced by primary antibody diluted in antibody diluent to the appropriate concentration. Negative control sections were treated with antibody diluent without antibody. Sections were incubated at room temperature for 1 h then washed 3 times in wash buffer. Universal Biotinylated Secondary Antibody (Vector R.T.U. kit) was added for 30 min, sections were washed in wash buffer twice then incubated with Vectastain Elite

ABC Reagent (Vector R.T.U. kit) for 30 min. Sections were washed 3 times with wash buffer then incubated for 5 min with DAB solution before being washed in running water for 5 min. The clinical samples labelled for p63, FBXW7 and MDM2 were reviewed by three independent scorers, blinded to any clinical details of the patients.

Immunofluorescence staining of tissue sections. Paraffin-embedded tissue samples of melanoma patients before and after acquisition of MAPKi resistance were kindly provided by Dr Christian Posch. After hydration of paraffin-embedded tissue in a xylene-alcohol series antigen-retrieval was done in Citric Buffer and left to cool down to room temperature. Samples were washed, covered by blocking buffer in a humidity chamber and then incubated with primary antibodies (MART-1 from Signalway Ab and SFI-6 against p63 from DSC Diagnostics Germany), diluted in blocking buffer and incubated over night at 4°C in a humidity chamber. The next day, excess primary antibody was removed with 3 washes and samples were incubated with the appropriate fluorophore-coupled secondary antibody, against the antigen of the primary antibody (1:800 in Blocking Buffer, 1.5h, RT). This was followed by 3 washes and the staining of the nuclei with 4', 6-diamidino-2-phenylindole (DAPI) (1:1000 in PBS, 5 min, RT). Excess DAPI was removed with one wash in PBS (5min, RT). Coverslips were mounted on the slides with the sections using Immu-Mount (Thermofisher) to preserve the immunofluorescence staining. Images of stained samples were then acquired with an INCell 2200 automated microscope using both 4x and 20x objectives. 4x objective fields were taken with a 15% overlap to allow image stitching and to provide a section overview. All images have been contrasted based on a negative control.

Immunocytochemistry. Cells were seeded onto coverslips and fixed the following day in 4% formaldehyde for 10 min followed by two 5 min washes in PBS. Cell membranes were permeabilised in 0.3% Triton X-100 for 2 min at RT coverslips were then washed twice with PBS. Cells were incubated with 5% goat serum/PBS for 30 min. After removal of the serum, cells were incubated with primary antibody diluted in 5% goat serum/PBS overnight at 4°C. Cells were washed 3 times for 10 min in PBS before being incubated with secondary antibody dilution 1/500 in 5% PBS/goat serum) for 1h at RT in the dark. Cells were washed twice for 10

min in PBS then incubated with 4',6-diamidino-2-phenylindole (DAPI) for 10 min followed by two washes in PBS for 10 min. Coverslips were mounted onto a glass slide and stored at 4˚C protected from light.

Annexin-V Binding assay. To induce apoptosis, cells were treated with different drugs for 24 h. After treatment adherent cells and any cells in supernatants were collected and pelleted before being washed in PBS. Cells were resuspended in 400µl 1X Becton Dickinson Annexin V Binding Buffer (BD Pharmingen™) and processed according to the manufacturer's instructions. Results were analysed using the Becton Dickinson FACSDiva software.

RESULTS

p63 expression significantly correlates with BRAF and NRAS mutational status in melanoma.

We have previously shown that expression of oncogenic p63 correlates with worse outcome in melanoma (7), but the association between p63 expression and BRAF/NRAS mutational status has not yet been established. A panel of 50 melanomas previously analysed for p63 expression (Figure 1A) were macro-dissected and genotyped for BRAF (exon 15) and NRAS (exons 2-3) mutational status. We identified a significant correlation between p63 expression and mutation in BRAF and NRAS (Figure 1B and Table1), supporting a similar correlation in established melanoma cell lines at both gene (Suppl Figure S1B) and protein levels (Figure 1C). Validation with an independent melanoma dataset from The Cancer Genome Atlas (TCGA) (43) confirmed an association (although not statistically significant) between increased p63 expression and BRAF and NRAS mutational status (Suppl Figure S1A).

In order to test whether p63 expression affects MAPK activation, p63 isoforms were transiently expressed in p63 null melanoma cell lines (Mel 224 and LM1) and resulted in increased expression of phosphorylated MEK1/2 (Figure 1D). Conversely silencing of endogenous p63 in a $BRAFV^{600E}$ melanoma cells (A375M) significantly reduced expression of phosphorylated MEK1/2 (Figure 1E). Overexpression of p63 ΔNβ isoform in WM164 cells significantly increased EGFR expression and affected phosphorylation activity. EGFR upregulation,

already reported in melanoma cell lines resistant to BRAF inhibition (44), resulted in increased phosphorylated MEK1/2 expression (Figure 1F). EGFR inhibition abolished p63-driven effects on phospho-MEK1/2 expression, suggesting that p63 can influence MAPK signalling via EGFR in melanoma cells.

Development and characterization of MAPK inhibitor resistant cell lines.

Cellular models were established to investigate the consequences of p63 expression in MAPKi-resistant melanomas. Five BRAF-inhibitor (BRAFi) resistant (WM1158, WM793, A375M, WM278 and WM164) and 2 MEK inhibitor (MEKi) resistant (A375M, WM164) melanoma cell lines were chronically treated three times a week for 10-12 weeks with 2μM PLX4032 (vemurafenib) and 50nM trametinib, respectively, until they acquired resistance. Major changes in cell shape, plasticity and size were observed: WM793-PLX and WM278-PLX cells became very elongated and acquired phenotypic features of mesenchymal cells; conversely WM1158-PLX cells transformed from mesenchymal-like to an epithelial-like morphology (Suppl. Figure S1C). Trametinib-resistant cells increased their size and become very large and multinucleated. These morphological changes were driven by a cytoskeleton reorganization with significant changes in actin fibers polarization and angle dispersion (Suppl. Fig S1D-E). To confirm the acquisition of BRAF or MEK inhibitor resistance, cells were treated with vemurafenib (3μM and 6μM) or with trametinib (50nM) for 24h. Expression of phosphorylated MEK and ERK was significantly decreased in BRAFi and MEKi sensitive cell lines whereas high dose vemurafenib or trametinib had no effect on MEK and ERK phosphorylation in MAPKi resistant cells (Figure 2A-C and Suppl. Figure S1F-G).

Resistance to BRAF inhibitors was further tested by measuring cell viability of resistant and sensitive cell lines after 24 hours of increasing concentration of vemurafenib. All cell lines tested showed significantly increased cell survival with vemurafenib compared to their sensitive counterpart (Figure 2D). Growth curves revealed significant lower cell proliferation in BRAFi and MEKi resistant cells (Figure 2E and Suppl. Figure S1H). High expression levels of CD271 have been associated with metastatic progression, enhanced survival, resistance to

MAPK inhibitors (45) and these cells also displayed enrichment of CD271 expression (Figure 2F and Suppl Figure S1I) when compared with their parental non-resistant cell lines.

Upregulated p63 expression contributes to development of MAPKi resistance in melanoma.

To investigate the impact of p63 expression in MAPKi resistant melanoma cells. Q-PCR analysis was performed using specific primers designed to detect all isoforms of TAp63 and ΔNp63 isoforms (7). TP63 mRNA expression was compared to normal primary human melanocytes (NHEM), which confirmed lack of detectable TA and ΔN p63 expression. Q-PCR analysis of TA and ΔN p63 showed an overall significant upregulation of both isoforms in all our melanoma MAPKi resistant cell lines (Figure 3A and Suppl figure S2A). Similar results were observed when p63 protein expression was measured: p63 isoforms were either upregulated in a cell specific manner or their expression was only increased in MAPKi resistant cells (Figures 3B-D and Suppl. Figure S2B). We further confirmed p63 upregulation at RNA and protein level in an independent panel of BRAFi-resistant melanoma cell lines (Figure 3A and C).

In order to determine whether increased p63 expression is sufficient to affect cell survival we used RNA interference specifically targeting p63 expression in melanoma cells. Western blot analysis showed that both shRNA sequences reduced endogenous expression of ΔNp63β protein in A375M cells compared to vector control (Figure 3E). Cells depleted of p63 were subsequently exposed to vemurafenib demonstrating significant reduction in cell viability when compared with control cells (Figure 3F). Similarly, BRAFi resistant cells infected with p63 shRNAs showed significant decrease in cell viability upon exposure to increasing doses of vemurafenib (Figure 3G and Suppl Figure S2C), demonstrating that reduction of p63 expression restores sensitivity to MAPKi treatment. Reactivation of p63 expression was also detected in melanoma samples from patients who developed resistance to combined BRAFi and MEKi (figure 3H and Supp.S2D-E).

Proteasomal degradation influences p63 stability in melanoma cells.

To examine regulation of p63 isoform stability in melanoma, established melanoma cell lines were treated with the peptide aldehyde inhibitor MG-132 (2μM) for 8h. Western blotting analysis showed stabilisation of endogenous p63 protein expression suggesting that proteasomal degradation may be one possible mechanism controlling p63 protein stability in melanoma cells (Figure 4A). Given the data supporting proteasome-mediated degradation of p63 in keratinocytes, we investigated E3-ubiquitin ligases in relation to p63 degradation in melanoma cells. Expression of ITCH is heterogeneous and does not always inversely correlate with p63 expression (Suppl Figure S3A), suggesting that its interaction with p63 in melanoma might only occur in a cell-type specific manner. Moreover, western blotting analysis showed no significant changes in ITCH expression in BRAFi resistant melanoma cell lines despite consistent upregulation of p63 isoforms (Suppl Figure S3B). We therefore investigated an alternative E3 ubiquitin ligase, namely FBXW7. Protein analysis revealed FBXW7β is the main isoform expressed in several established melanoma cell lines regardless of BRAF mutational status (Suppl Figure S3C). Isoform-specific Q-PCR analysis (alpha, beta and gamma FBXW7), showed significant reduction in FBXW7β isoforms in resistant cells (Figure 4B and Suppl Figure S3D). Similarly, western blotting analysis showed significant downregulation of FBXW7 protein in all MAPKi resistant cells (Figure 4C-D). Immunofluorescence staining of FBXW7 protein in WM1158 and WM793 cells revealed that in both parental and BRAFi resistant cells, FBXW7β is predominantly localized to the nucleus (Figure 4E and Suppl Figure S3E). Sub-cellular fractionation experiments confirmed this nuclear localization in all melanoma cell lines, and also revealed significantly reduced FBXW7β expression in BRAFi resistant cells (Figure 4F). Our data therefore demonstrate that melanoma expresses FBXW7β protein which is mainly confined to the nucleus.

Downregulated FBXW7 mRNA and protein in MAPKi resistant cells suggested a possible downstream effect of MAPK signalling on FBXW7. Pancreatic cancer samples with NRAS mutation displayed higher ERK activation leading to decreased FBXW7 expression with ERK found to directly phosphorylate FBXW7 at the Thr205 residue and regulate protein stability via proteasomal degradation (46). To investigate this in melanoma, A375M and WM793

melanoma cells were treated with vemurafenib for 24 hours. In contrast to BRAFi resistant cells, transient incubation of melanoma cells with vemurafenib did not show any significant reduction of endogenous expression of FBXW7 (Suppl Figure S3F) suggesting that FBXW7 protein stability in melanoma cells does not rely solely on ERK phosphorylation.

Using specific antibodies against FBXW7, immunoprecipitation experiments in few melanoma cell lines demonstrated direct protein interaction between endogenous ΔNp63 and FBXW7 (Figure 4G). FBXW7 interaction occurs with all p63 isoforms (Figure 4H). To further confirm the direct relationship between FXBW7 and p63 protein, FBXW7 shRNAs knockdown experiments were performed: in A375M melanoma cells, p63 protein levels were significantly upregulated only in the cells with FBXW7 knockdown (Figure 4I).

Expression and location of mdm2 influence p63/FBXW7 interaction in MAPKi treated melanoma

In keratinocytes, MDM2 and FBXW7 cooperatively control stability of p63 protein following differentiation and UV irradiation. MDM2 transports ΔNp63 into the cytoplasm where, upon interaction with the phosphodegron motif of FBXW7, it undergoes proteasomal degradation (17). Interaction between FBXW7 and MDM2 has not been systematically assessed in any other cellular systems and in order to test whether this model is also relevant in melanoma, we examined patterns of expression and localization of MDM2 and FBXW7. Primary melanomas showed strong nuclear reactivity of FBXW7 in both tumour and epidermal keratinocytes, while MDM2 distribution was cytoplasmic and nuclear with slight reactivity within basal layer of epidermis (Figure 5A). To further analyse cytoplasmic and nuclear reactivity for MDM2 and FBXW7, 31 and 24 primary melanoma tumour nests respectively were analysed in 7 clinical samples. Significantly higher MDM2 reactivity was present in the cytoplasm compared to the nucleus, while the reverse trend was observed for FBXW7. This inverse correlation between MDM2 and FBXW7 expression was further observed at the gene level in a TCGA SKCM dataset of skin cutaneous melanoma (Suppl fig. S4A). To investigate the effect of resistance on MDM2 expression, mdm2 mRNA and protein levels were compared in MAPKi-sensitive

and resistant cell lines. Mdm2 mRNA and protein was significantly elevated in most established MAPKi resistant cell lines (Figure 5B-D), whereas no significant changes were observed in most cell lines for MDM4 (Figure 5C). MDM2 was mainly localized to the nucleus in immunofluorescence experiments and, in MAPKi resistant cell lines the intensity of fluorescence was increased significantly (Figure 5E and suppl figure S4B-C). Sub-cellular fractionation experiments confirmed nuclear enrichment of MDM2 expression in most MAPKi-resistant melanoma cells (Figures 5F-G).

To explore whether MDM2 expression and localization reflected a potential interaction with nuclear FBXW7 we undertook immunoprecipitation experiments in WM793, A375M melanoma cells and HaCaT keratinocytes which confirmed protein-protein interactions between MDM2 and FBXW7 in melanoma cell lines (Figure 5H) and HaCaT keratinocytes. In vitro ubiquitylation experiment shows that mdm2 is able to increase FBXW7 ubiquitylation (Figure 5I). To further investigate the consequence of this interaction, MDM2 was overexpressed in melanoma cells to test the effect on FBXW7 protein expression levels. Transfected cells were treated with the proteasome inhibitor MG132 (2μM) 40 hours post-transfection and cells harvested after 8 hours of MG132 treatment. Western blotting revealed that exogenously overexpressed MDM2 reduced FBXW7 protein in the absence of MG132, (Figure 5J and Suppl Figure S4D), and this downregulation was rescued by proteasome inhibition. The effect on FBXW7 was specific for MDM2 rather than MDM4 which, upon over-expression, failed to reduce endogenous FBXW7 (Suppl Figure S4E).

Nutlin-3A degrades p63 expression and sensitizes MAPKi-resistant melanoma cells to apoptosis.

Having established that MAPKi resistance in melanoma cells results in p63 upregulation, we next investigated whether p63 inhibition might restore chemosensitivity in MAPKi resistant cells. As few inhibitors of p63 expression are currently available, we adopted an indirect approach and tested the effects on p63 expression of molecules targeting other p63 regulators. Nutlin-3A, an MDM2-p53 interaction inhibitor, induces p53 re-activation. Nutlin-3A

inhibits p73 interactions with MDM2 and MDM4, but does not have an inhibitory effect on TA and ΔNp63 (47). To test whether Nutlin-3A could affect p63 expression, MAPKi sensitive and resistant cells were treated with increasing doses of Nutlin-3A. There was a dose dependent reduction in p63 protein expression by Western blotting in most cellular model tested. In A375M cells, treatment with Nutlin-3A reduced ΔNp63β protein expression in a dose dependent manner (Suppl Figure S5A). Interestingly, Nutlin-3A was able to affect the stability of several p63 isoforms, as seen in the WM793 cells (Figure 6A). In addition, Nutlin-3A treatment also reduced all p63 isoform in WM793-PLX cells (Figure 6B) and in A375M-TR (Figure 6C). This is the first evidence that Nutlin-3A inhibits p63 expression in melanoma and N-TERT human immortalized keratinocytes (Suppl Figure S5B). Since no significant changes were detected at mRNA level in p63 TA and ΔN isoforms in either parental or resistant cells (Figure 6D, and Suppl Figure S5C), this suggests that Nutlin-3A only affects p63 protein stability. After Nutlin-3A treatment, most melanoma cell lines showed significant downregulation of ITCH protein (Suppl Figure S5D) but increased FBXW7 protein expression in a dose dependent manner (Figure 6E-F, Suppl Figure S5E). These observations provide further support for the hypothesis that p63 protein stability is specifically controlled by FBXW7 in melanoma cells. Similarly, Nutlin-3A induced 10 and 15-fold increased transcriptional expression of FBXW7 mRNA in A375M and WM793 cells, respectively, particularly the FBXW7β isoform (Figure 6G, Suppl Figure S5F).

Previous evidence has revealed the existence of a p53 binding site in exon 1b of the FBXW7 promoter and expression of endogenous FBXW7β, but not FBXW7α, was previously shown to be induced in a p53-dependent manner (48). In order to establish whether FBXW7 upregulation after Nutlin-3A treatment was p53-mediated, melanoma cells were transfected with specific siRNA against p53. In the absence of p53, Nutlin-3A had no effect on FBXW7 expression suggesting that Nutlin-3A mediated upregulation of FBXW7 may be dependent on p53 stabilization (Figure 6H). This was further supported by the inability of Nutlin-3A to degrade p63 expression in a couple of p53 mutant melanoma cell lines (CHL-1 and SK-MEL-28) (figure 6I and Suppl. Figure S5G). We further investigated whether the effect of mdm2

inhibition in melanoma cells in combination with MAPK inhibitors could synergistically increase cell death. Melanoma cell lines were treated with vemurafenib, Trametinib or Nutlin-3A as well as RG7112 and AMG232 alone or in combination. Apoptosis induction was significantly higher with combined treatment for 24 hours (Figure 6J and Suppl Figure S5H). Taken together, these data highlight the involvement of p63 upregulation in MAPKi resistance and suggest a potential therapeutical approach to prevent it by combining BRAF and/or MEK inhibition with Nutlin-3A or an alternative mdm2 inhibitory treatment.

DISCUSSION

We have previously reported p63 protein expression in more than 50% of melanomas irrespective of tumour stage (7). Here we further analysed mutational status of BRAF and NRAS in a subset of tumours previously scored for p63 expression establishing a statistically significant correlation between p63 expression and BRAF or NRAS mutation. Although our results raised the possibility of an association between p63 and MAPK, a direct link between the two signalling pathways has never been established.

p63 upregulation has been reported in another skin malignancy - cutaneous squamous cell carcinoma (49-53). In keratinocytes tyrosine kinase receptor EGFR has been implicated in regulating ΔNp63 expression by several signalling mechanisms including via phosphoinositide-3-kinase (PI3K) pathway (52). Here we showed that in melanoma cells, ectopic overexpression of p63 isoforms in BRAF wild type cell lines in conjunction with knockdown of p63 in $BRAF^{V600E}$ mutated cell lines resulted in upregulation and downregulation, respectively, of the MAPK signalling cascade. Therefore, in melanoma, p63 expression may positively affect MAPK signalling via EGFR, although further experiments are needed to elucidate exact mechanisms by which p63 could regulate phosphorylation of MEK1/2 in melanoma.

In order to investigate the functional relevance of p63 expression on MAPKi resistance development, we established an *in vitro* model by generating BRAFi and MEKi resistant melanoma cell lines. To date, multiple MAPKi resistance mechanisms have been identified

and include emergence of NRAS or MEK mutation, drug resistant splice variant of BRAF, increased expression of MAP3K, COT, cyclin D1, AEBP1 and several growth factor receptors including IGFR, PDGFR (54-58). Once our cells acquired resistance, drastic changes in cell shape, plasticity and size were observed (59). Chronically treated cells become more resistant to BRAF or MEK inhibition with reduced apoptosis induction compared to sensitive parental cell lines. Similar findings have been corroborated by other groups (60). Enrichment of CD271 was recently shown in BRAFi resistant melanoma cells (61,62). Analysis of our MAPKi resistant cell lines confirmed significant upregulation of CD271 expression, although with variation across cell lines. Aberrant activation of the MAPK signalling significantly upregulated p63 mRNA and protein expression in our cellular models and in 2 out of 3 clinical samples from patients with acquired MAPKi resistance. Whilst such observed p63 changes could be downstream effects of MAPKi, they may represent a driving mechanism for BRAF inhibitor resistance.

We previously showed that p63 has an anti-apoptotic role in melanoma and confers resistance to chemotherapy (7). Depletion of p63 by RNA interference results in activation of p53 dependent mitochondrial apoptotic pathways, rendering melanoma cells sensitive to chemotherapies as well as to vemurafenib treatment. Consistent with these results, A375M cells depleted of p63 and treated with vemurafenib demonstrated significantly decreased cell survival. Furthermore, p63 depletion in BRAFi resistant cells, re-sensitized these cells to vemurafenib and enhanced apoptosis. These results suggest that survival role of p63 is enhanced in cells chronically treated with vemurafenib.

In order to understand the impact of p63 upregulation in MAPKi resistance we explored regulation of p63 expression in melanoma cells. Treatment with the proteasome inhibitor MG132, stabilized p63 isoforms suggesting p63 stability in melanoma is controlled by an E3 ubiquitin ligase. E3 ubiquitin ligases such as ITCH, FBXW7, WWP1 and Pirh2 have been extensively explored in keratinocytes and shown to regulate p63 protein and differentiation (11,15,16,17). Only FBXW7β was significantly reduced when E3 ubiquitin ligases expression were compared in MAPKi sensitive and resistant cells to identify potential regulators of p63

stability. In keratinocytes, MDM2 and FBXW7 can cooperatively control the stability of p63 protein upon keratinocytes differentiation and UV irradiation. MDM2 transports ΔNp63 into the cytoplasm where it interacts with FBXW7 via phosphodegron motif and degrades it via proteasomal degradation pathway (15). More recently was shown that HDACi also reduces ΔNp63 protein level via FBXW7 (19). Using immunoprecipitation experiments, we have demonstrated the endogenous interaction between p63 and FBXW7 in melanoma cells whereby stable depletion of FBXW7 resulted in upregulation of p63 protein.

P53 mutations are less common in melanoma compared to other skin cancers (34,62), but MDM2 is often overexpressed in melanoma and recognized as one of the potential causes of p53 inactivity in melanoma cells (36,63,64). FBXW7 was found to be mutated in melanoma samples with frequent downregulation of its expression (18). Based on these observations we hypothesized that FBXW7 downregulation could be either the direct result of the lack of its transcriptional activation by p53, which is degraded by high levels of MDM2 in melanoma or because of a direct interaction between the two. No evidence for an interaction between MDM2 and FBXW7 has previously been reported for any cell type. We analysed an independent cohort of melanoma clinical samples (TCGA SKCM) dataset for MDM2 and FBXW7 mRNA expression, and the data at the gene level matched our staining expression pattern, confirming the inverse relationship observed in our established cell lines. Further analysis of MDM2 expression revealed nuclear MDM2 enrichment in MAPKi resistant cells and immunoprecipitation experiments confirmed endogenous interaction of MDM2 with FBXW7.

To support our model, inhibition of MDM2 activity by Nutlin-3A, resulted in increased FBXW7 expression and decreased p63 protein. Although it is possible that MDM2 overexpression could reduce FBXW7 protein via p53 downregulation, direct interaction between the two suggests that this is less likely. These results provide evidence of a previously unreported mechanism by which MDM2 can increase ubiquitylation activity and regulate FBXW7 protein stability in melanoma, ultimately affecting p63 expression.

Taken together, these data suggested that chronic treatment with MAPK inhibitors results in nuclear mdm2 enrichment with consequent FBXW7 protein downregulation. p63 accumulates as a result of failure of FBXW7-mediated degradation and overexpression of p63 contributes to increased cell survival and resistance to MAPK inhibitors (cartoon A). Although complete therapeutic knockdown of p63 would be challenging, indirect pharmacologic inhibition of p63 function might reduce MAPKi resistance and potentially improve survival outcome. In this regard, we propose that use of nutlin-3A during treatment with MAPKi targeted therapy would synergistically induce apoptosis and suppress melanoma growth, thereby abrogating MAPKi resistance (65) (cartoon B). Our data unveil a novel survival role of p63 in melanoma and provide an approach to abrogate or overcome acquired resistance of melanoma to MAPK inhibitor targeted therapy.

Acknowledgments and Ethics. We are grateful to Dr Gary Warnes, Flow Cytometry Core Facility Manager, for technical advice, to Rebecca Carroll and Laura Neal for the assistance with the tissue samples immunostaining, Dr Belen Martin and Dr Jan Soetaert for the technical support with fluorescence microscopy. Funding support was provided by British Skin Foundation for AP (6063s to DB) and VM (016/s/16 to TM), Barts and The London Charity (458/1494 to DB and CAH), EC Erasmus+ for LFG (2017-SMP-P-211) and AIRC for EV (IG 17462 to MR).

REFERENCES

1. Flaherty KT, Puzanov I, Kim KB, Ribas A, McArthur GA, Sosman JA*, et al.* Inhibition of mutated, activated BRAF in metastatic melanoma. N Engl J Med **2010**;363:809-19
2. Long GV, Stroyakovskiy D, Gogas H, Levchenko E, de Braud F, Larkin J*, et al.* Combined BRAF and MEK Inhibition versus BRAF Inhibition Alone in Melanoma. New England Journal of Medicine **2014**;371:1877-88
3. Long GV, Fung C, Menzies AM, Pupo GM, Carlino MS, Hyman J*, et al.* Increased MAPK reactivation in early resistance to dabrafenib/trametinib combination therapy of BRAF-mutant metastatic melanoma. Nature communications **2014**;5:5694
4. Koster MI, Kim S, Mills AA, DeMayo FJ, Roop DR. p63 is the molecular switch for initiation of an epithelial stratification program. Genes & development **2004**;18:126-31
5. Ribeiro-Silva A, Zambelli Ramalho LN, Britto Garcia S, Zucoloto S. The relationship between p63 and p53 expression in normal and neoplastic breast tissue. Archives of pathology & laboratory medicine **2003**;127:336-40
6. Fukushima N, Satoh T, Sueoka N, Sato A, Ide M, Hisatomi T*, et al.* Clinico-pathological characteristics of p63 expression in B-cell lymphoma. Cancer science **2006**;97:1050-5

7. Matin NR, Anissa C, Stephanie C, David M, Manuela G, Paolo S*, et al.* p63 is an alternative p53 repressor in melanoma that confers chemoresistance and a poor prognosis. The Journal of Experimental Medicine **2013**;210:581-603
8. Bakkers J, Camacho-Carvajal M, Nowak M, Kramer C, Danger B, Hammerschmidt M. Destabilization of DeltaNp63alpha by Nedd4-mediated ubiquitination and Ubc9-mediated sumoylation, and its implications on dorsoventral patterning of the zebrafish embryo. Cell cycle (Georgetown, Tex) **2005**;4:790-800
9. Leonard MK, Hill NT, Grant ED, Kadakia MP. DeltaNp63alpha represses nuclear translocation of PTEN by inhibition of NEDD4-1 in keratinocytes. Archives of dermatological research **2013**;305:733-9
10. Fomenkov A, Zangen R, Huang Y-P, Osada M, Guo Z, Fomenkov T*, et al.* RACK1 and stratifin target DeltaNp63alpha for a proteasome degradation in head and neck squamous cell carcinoma cells upon DNA damage. Cell cycle (Georgetown, Tex) **2004**;3:1285-95
11. Rossi M, Aqeilan RI, Neale M, Candi E, Salomoni P, Knight RA*, et al.* The E3 ubiquitin ligase Itch controls the protein stability of p63. Proceedings of the National Academy of Sciences of the United States of America **2006**;103:12753-8
12. Yang F, Tay KH, Dong L, Thorne RF, Jiang CC, Yang E*, et al.* Cystatin B inhibition of TRAIL-induced apoptosis is associated with the protection of FLIP(L) from degradation by the E3 ligase itch in human melanoma cells. Cell death and differentiation **2010**;17:1354-67
13. Coppari E, Yamada T, Bizzarri AR, Beattie CW, Cannistraro S. A nanotechnological, molecular-modeling, and immunological approach to study the interaction of the anti-tumorigenic peptide p28 with the p53 family of proteins. International journal of nanomedicine **2014**;9:1799-813
14. Yin Q, Han T, Fang BA-O, Zhang G, Zhang C, Roberts ER*, et al.* K27-linked ubiquitination of BRAF by ITCH engages cytokine response to maintain MEK-ERK signaling. Nature communications **2019**;10:1870.
15. Li Y, Zhou Z, Chen C. WW domain-containing E3 ubiquitin protein ligase 1 targets p63 transcription factor for ubiquitin-mediated proteasomal degradation and regulates apoptosis. Cell death and differentiation **2008**;15:1941-51
16. Jung YS, Qian Y, Yan W, Chen X. Pirh2 E3 Ubiquitin Ligase Modulates Keratinocyte Differentiation Through p63. The Journal of investigative dermatology **2013**;133:1178-87
17. Galli F, Rossi M, D'Alessandra Y, De Simone M, Lopardo T, Haupt Y*, et al.* MDM2 and Fbw7 cooperate to induce p63 protein degradation following DNA damage and cell differentiation. Journal of cell science **2010**;123:2423-33
18. Aydin IT, Melamed RD, Adams SJ, Castillo-Martin M, Demir A, Bryk D*, et al.* FBXW7 mutations in melanoma and a new therapeutic paradigm. Journal of the National Cancer Institute **2014**;106:dju107-dju
19. Napoli M, Venkatanarayan A, Raulji P, Meyers BA, Norton W, Mangala LS*, et al.* DeltaNp63/DGCR8-Dependent MicroRNAs Mediate Therapeutic Efficacy of HDAC Inhibitors in Cancer. Cancer cell **2016**;29:874-88
20. Strohmaier H, Spruck CH, Kaiser P, Won KA, Sangfelt O, Reed SI. Human F-box protein hCdc4 targets cyclin E for proteolysis and is mutated in a breast cancer cell line. Nature **2001**;413:316-22
21. Koepp DM, Schaefer LK, Ye X, Keyomarsi K, Chu C, Harper JW*, et al.* Phosphorylation-dependent ubiquitination of cyclin E by the SCFFbw7 ubiquitin ligase. Science (New York, NY) **2001**;294:173-7
22. Spruck C, Strohmaier HM. Seek and Destroy: SCF Ubiquitin Ligases in Mammalian Cell Cycle Control. Cell cycle (Georgetown, Tex) **2002**;1:248-52
23. Welcker M, Orian A, Grim JE, Eisenman RN, Clurman BE. A nucleolar isoform of the Fbw7 ubiquitin ligase regulates c-Myc and cell size. Current biology : CB **2004**;14:1852-7
24. Ye X, Nalepa G, Welcker M, Kessler BM, Spooner E, Qin J*, et al.* Recognition of phosphodegron motifs in human cyclin E by the SCF(Fbw7) ubiquitin ligase. The Journal of biological chemistry **2004**;279:50110-9

25. Mo J-S, Ann E-J, Yoon J-H, Jung J, Choi Y-H, Kim H-Y*, et al.* Serum- and glucocorticoid-inducible kinase 1 (SGK1) controls Notch1 signaling by downregulation of protein stability through Fbw7 ubiquitin ligase. Journal of cell science **2011**;124:100-12
26. Schulein C, Eilers M, Popov N. PI3K-dependent phosphorylation of Fbw7 modulates substrate degradation and activity. FEBS letters **2011**;585:2151-7
27. Min S-H, Lau AW, Lee TH, Inuzuka H, Wei S, Huang P*, et al.* Negative regulation of the stability and tumor suppressor function of Fbw7 by the Pin1 prolyl isomerase. Molecular cell **2012**;46:771-83
28. Welcker M, Larimore EA, Swanger J, Bengoechea-Alonso MT, Grim JE, Ericsson J*, et al.* Fbw7 dimerization determines the specificity and robustness of substrate degradation. Genes & development **2013**;27:2531-6
29. Kubbutat MH, Jones SN, Vousden KH. Regulation of p53 stability by Mdm2. Nature **1997**;387:299-303
30. Haupt Y, Maya R, Kazaz A, Oren M. Mdm2 promotes the rapid degradation of p53. Nature **1997**;387:296-9
31. Huang L, Yan Z, Liao X, Li Y, Yang J, Wang ZG*, et al.* The p53 inhibitors MDM2/MDMX complex is required for control of p53 activity in vivo. Proceedings of the National Academy of Sciences of the United States of America **2011**;108:12001-6
32. Leslie PL, Ke H, Zhang Y. The MDM2 RING domain and central acidic domain play distinct roles in MDM2 protein homodimerization and MDM2-MDMX protein heterodimerization. The Journal of biological chemistry **2015**;290:12941-50
33. Schwaederle M, Elkin SK, Tomson BN, Carter JL, Kurzrock R. Squamousness: Next-generation sequencing reveals shared molecular features across squamous tumor types. Cell cycle (Georgetown, Tex) **2015**;14:2355-61
34. Hodis E, Watson IR, Kryukov GV, Arold ST, Imielinski M, Theurillat J-P*, et al.* A landscape of driver mutations in melanoma. Cell **2012**;150:251-63
35. Polsky D, Melzer K, Hazan C, Panageas KS, Busam K, Drobnjak M*, et al.* HDM2 protein overexpression and prognosis in primary malignant melanoma. J Natl Cancer Inst **2002**;94:1803-6
36. Muthusamy V, Hobbs C, Nogueira C, Cordon-Cardo C, McKee PH, Chin L*, et al.* Amplification of CDK4 and MDM2 in malignant melanoma. Genes, chromosomes & cancer **2006**;45:447-54
37. Gembarska A, Luciani F, Fedele C, Russell EA, Dewaele M, Villar S*, et al.* MDM4 is a key therapeutic target in cutaneous melanoma. Nat Med **2012**;18:1239-47
38. Lu M, Breyssens H, Salter V, Zhong S, Hu Y, Baer C*, et al.* Restoring p53 function in human melanoma cells by inhibiting MDM2 and cyclin B1/CDK1-phosphorylated nuclear iASPP. Cancer cell **2013**;23:618-33
39. Vassilev LT, Vu BT, Graves B, Carvajal D, Podlaski F, Filipovic Z*, et al.* In vivo activation of the p53 pathway by small-molecule antagonists of MDM2. Science **2004**;303:844-8
40. Lau LM, Nugent JK, Zhao X, Irwin MS. HDM2 antagonist Nutlin-3 disrupts p73-HDM2 binding and enhances p73 function. Oncogene **2008**;27:997-1003
41. Tisato V, Voltan R, Gonelli A, Secchiero P, Zauli G. MDM2/X inhibitors under clinical evaluation: perspectives for the management of hematological malignancies and pediatric cancer. Journal of hematology & oncology **2017**;10:133
42. Worrall C, Suleymanova N, Crudden C, Trocoli Drakensjo I, Candrea E, Nedelcu D*, et al.* Unbalancing p53/Mdm2/IGF-1R axis by Mdm2 activation restrains the IGF-1-dependent invasive phenotype of skin melanoma. Oncogene **2017**;36:3274-86
43. Cancer-Genome-Atlas-Network. Genomic Classification of Cutaneous Melanoma. Cell **2015**;161:1681-96

44. Girotti MR, Pedersen M, Sanchez-Laorden B, Viros A, Turajlic S, Niculescu-Duvaz D*, et al.* Inhibiting EGF Receptor or SRC Family Kinase Signaling Overcomes BRAF Inhibitor Resistance in Melanoma. Cancer discovery **2013**;3:158
45. Restivo G, Diener J, Cheng PF, Kiowski G, Bonalli M, Biedermann T*, et al.* Publisher Correction: The low affinity neurotrophin receptor CD271 regulates phenotype switching in melanoma. Nature communications **2018**;9:314
46. Ji S, Qin Y, Shi S, Liu X, Hu H, Zhou H*, et al.* ERK kinase phosphorylates and destabilizes the tumor suppressor FBW7 in pancreatic cancer. Cell research **2015**;25:561-73
47. Leao M, Gomes S, Bessa C, Soares J, Raimundo L, Monti P*, et al.* Studying p53 family proteins in yeast: induction of autophagic cell death and modulation by interactors and small molecules. Experimental cell research **2015**;330:164-77
48. Kimura T, Gotoh M, Nakamura Y, Arakawa H. hCDC4b, a regulator of cyclin E, as a direct transcriptional target of p53. Cancer science **2003**;94:431-6
49. Hibi K, Trink B, Patturajan M, Westra WH, Caballero OL, Hill DE*, et al.* AIS is an oncogene amplified in squamous cell carcinoma. Proceedings of the National Academy of Sciences of the United States of America **2000**;97:5462-7
50. Wu N, Rollin J, Masse I, Lamartine J, Gidrol X. p63 regulates human keratinocyte proliferation via MYC-regulated gene network and differentiation commitment through cell adhesion-related gene network. The Journal of biological chemistry **2012**;287:5627-38
51. Missero C, Antonini D. p63 in Squamous Cell Carcinoma of the Skin: More Than a Stem Cell/Progenitor Marker. The Journal of investigative dermatology **2017**;137:280-1
52. Robinson DJ, Patel A, Purdie KJ, Wang J, Rizvi H, Hufbauer M*, et al.* Epigenetic Regulation of iASPP-p63 Feedback Loop in Cutaneous Squamous Cell Carcinoma. The Journal of investigative dermatology **2019**;139: 1658-71
53. Montagut C, Sharma SV, Shioda T, McDermott U, Ulman M, Ulkus LE*, et al.* Elevated CRAF as a potential mechanism of acquired resistance to BRAF inhibition in melanoma. Cancer research **2008**;68:4853-61
54. Corcoran RB, Dias-Santagata D, Bergethon K, Iafrate AJ, Settleman J, Engelman JA. BRAF gene amplification can promote acquired resistance to MEK inhibitors in cancer cells harboring the BRAF V600E mutation. Science signaling **2010**;3:ra84-ra84
55. Johannessen CM, Boehm JS, Kim SY, Thomas SR, Wardwell L, Johnson LA*, et al.* COT drives resistance to RAF inhibition through MAP kinase pathway reactivation. Nature **2010**;468:968-72
56. Poulikakos PI, Persaud Y, Janakiraman M, Kong X, Ng C, Moriceau G*, et al.* RAF inhibitor resistance is mediated by dimerization of aberrantly spliced BRAF(V600E). Nature **2011**;480:387-90
57. Hu W, Jin L, Jiang CC, Long GV, Scolyer RA, Wu Q*, et al.* AEBP1 upregulation confers acquired resistance to BRAF (V600E) inhibition in melanoma. Cell death & disease **2013**;4:e914-e
58. Kim MH, Kim J, Hong H, Lee SH, Lee JK, Jung E*, et al.* Actin remodeling confers BRAF inhibitor resistance to melanoma cells through YAP/TAZ activation. EMBO journal **2016**; 35:462-78.
59. Kosnopfel C, Sinnberg T, Sauer B, Niessner H, Schmitt A, Makino E*, et al.* Human melanoma cells resistant to MAPK inhibitors can be effectively targeted by inhibition of the p90 ribosomal S6 kinase. Oncotarget **2017**;8:35761-75
60. Lehraiki A, Cerezo M, Rouaud F, Abbe P, Allegra M, Kluza J*, et al.* Increased CD271 expression by the NF-kB pathway promotes melanoma cell survival and drives acquired resistance to BRAF inhibitor vemurafenib. Cell discovery **2015**;1:15030

61. Richard G, Dalle S, Monet MA, Ligier M, Boespflug A, Pommier RM*, et al.* ZEB1-mediated melanoma cell plasticity enhances resistance to MAPK inhibitors. EMBO molecular medicine **2016**;8:1143-61

62. Zerp SF, van Elsas A, Peltenburg LT, Schrier PI. p53 mutations in human cutaneous melanoma correlate with sun exposure but are not always involved in melanomagenesis. British journal of cancer **1999**;79:921-6

63. Polsky D, Bastian BC, Hazan C, Melzer K, Pack J, Houghton A*, et al.* HDM2 Protein Overexpression, but not Gene Amplification, is Related to Tumorigenesis of Cutaneous Melanoma. Cancer research **2001**;61:7642

64. Ji Z, Njauw CN, Taylor M, Neel V, Flaherty KT, Tsao H. p53 rescue through HDM2 antagonism suppresses melanoma growth and potentiates MEK inhibition. The Journal of investigative dermatology **2012**;132:356-64

65. Ji Z, Kumar R, Taylor M, Rajadurai A, Marzuka-Alcala A, Chen YE*, et al.* Vemurafenib synergizes with nutlin-3 to deplete survivin and suppresses melanoma viability and tumor growth. Clinical cancer research : an official journal of the American Association for Cancer Research **2013**;19:4383-91

TABLES

No.	Gender	Age	Body site	Type	Breslow Th.	P63 expression	BRAF status	NRAS status	Summary
1	M	36	Extremities (left shin)	Primary	T3	Positive	Wild type	G12D	NRAS mutated
2	F	72	Acral (right heel)	Primary	T4	Positive	V600E	Wild type	BRAF mutated
3	F	41	Trunk (back)	Primary	T2	Positive	V600E	Wild type	BRAF mutated
4	M	82	Trunk (lower back)	Primary	T3	Positive	V600E	Wild type	BRAF mutated
5	F	47	Head / neck	Primary	T2	Positive	V600E	Wild type	NRAS mutated
6	F	79	Extremities (calf)	Primary	T1	Positive	Wild type	Wild type	Wild type
7	F	56	Trunk (chest)	Primary	T1	Positive	Wild type	Wild type	Wild type
8	M	37	Trunk (abdomen)	Primary	T3	Positive	V600E	Wild type	BRAF mutated
9	F	71	Extremities (left forearm)	Primary	T4	Positive	V600K	Wild type	BRAF mutated
10	M	83	Extremities (calf)	Primary	T1	Negative	Wild type	Wild type	Wild type
11	M	21	Extremities (calf)	Primary	T2	Negative	Wild type	Wild type	Wild type
12	M	42	Trunk (back)	Primary	T3	Negative	Wild type	Wild type	Wild type
13	M	38	Head and neck (posterior)	Primary	T1	Positive	Wild type	Q61R	NRAS mutated
14	M	43	Trunk (left clavicle)	Primary	T1	Negative	Wild type	Wild type	Wild type
15	F	79	Extremities (right arm)	Primary	T1	Negative	Wild type	Q61L	NRAS mutated
16	F	42	Extremities (left arm)	Primary	T2	Positive	V600E	Wild type	BRAF mutated
17	F	70	Extremities (right lower leg)	Primary	T1	Positive	V600K	Wild type	BRAF mutated
18	F	56	Trunk (mid back)	Primary	T1	Negative	Wild type	Wild type	BRAF mutated
19	M	65	Trunk (back)	Primary	T3	Negative	Wild type	Wild type	Wild type
20	M	68	Trunk	Primary	T2	Positive	Wild type	Q61K	Wild type
21	F	65	Extremities (right shin)	Primary	T3	Positive	V600K	Wild type	NRAS mutated
22	M	68	Head and neck	Primary	T1	Negative	Wild type	Wild type	BRAF mutated
23	F	32	Extremities (left arm)	Primary	T1	Positive	Wild type	Wild type	Wild type
24	F	67	Extremities (right arm)	Recurrence		Positive	V600E	Wild type	NRAS mutated
25	F	65	Skin	Recurrence		Negative	Wild type	Q61R	Wild type
26	F	60	Skin (right sole)	Recurrence		Positive	Wild type	Wild type	Wild type
27	M	76	Skin (left foot)	Recurrence		Positive	Wild type	Wild type	Wild type
28	M	72	Skin (left upper arm)	Recurrence		Positive	Wild type	Q61R	NRAS mutated
29	F	64	Extremities (skin)	Metastatic		Positive	Wild type	Q61R	NRAS mutated
30	F	57	Parotid	Metastatic		Positive	V600E	Wild type	BRAF mutated
31	F	42	Lymph	Metastatic		Negative	Wild type	Wild type	Wild type
32	F	50	Lymph	Metastatic		Negative	Wild type	Wild type	Wild type
33	F	56	Skin (head and neck)	Metastatic		Positive	Wild type	Wild type	Wild type
34	F	36	Lymph	Metastatic		Negative	Wild type	Wild type	Wild type
35	M	37	Lymph	Metastatic		Positive	Wild type	Wild type	Wild type
36	M	60	Lymph	Metastatic		Positive	Wild type	Wild type	Wild type
37	F	59	Lymph (left groin)	Metastatic		Positive	Wild type	Wild type	Wild type
38	M	74	Lymph (right axilla)	Metastatic		Positive	Wild type	Wild type	Wild type
39	M	81	Lymph	Metastatic		Positive	Wild type	Q61R	NRAS mutated
40	M	50	Lymph (right neck)	Metastatic		Positive	V600E+K601del	Wild type	BRAF mutated
41	M	51	Lymph (supraclavicular)	Metastatic		Positive	V600E+K601del	Wild type	BRAF mutated
42	F	58	Lymph (right inguinal mass)	Metastatic		Positive	V600E	Wild type	BRAF mutated
43	F	58	Lymph (right groin)	Metastatic		Negative	Wild type	Wild type	Wild type
44	F	77	Lymph (groin)	Metastatic		Positive	Wild type	Q61R	NRAS mutated
45	M	52	Lymph (groin)	Metastatic		Negative	Wild type	Wild type	Wild type
46	M	86	Lymph (axilla)	Metastatic		Positive	V600K	Wild type	BRAF mutated
47	F	78	Lymph	Metastatic		Negative	Wild type	Q61R	NRAS mutated
48	M	37	Lymph (axilla)	Metastatic		Positive	Wild type	Q61K	NRAS mutated
49	F	42	Lymph	Metastatic		Negative	Wild type	Wild type	Wild type
50	F	57	Skin (nose)	Metastatic		Negative	Wild type	Wild type	Wild type

Table 1. Clinical features, p63 expression and BRAF/NRAS mutational status of melanoma samples. BRAF/NRAS mutated samples are represented in red. p63 expression was established by 3 independent scorers. Positive expression was considered when p63 average expression within the tumour displayed >50% positive reactivity.

FIGURE LEGENDS

Figure 1. Correlation of p63 expression and BRAF/NRAS mutational status in melanoma. (A) Representative images of p63 staining on primary melanoma lesions. Scale bar represents 50 μm magnified image scale bar. (B) 50 samples scored for % of p63 immunohistochemistry staining by 3 independent scorers were dewaxed and processed for DNA extraction. Each DNA sample (50ng) was amplified for BRAF (exon 15) and for NRAS (exons 2 and 3) by specific PCR. Scatter plots show significant correlation between p63

protein expression and BRAF/NRAS mutational status. (C) Western blot analysis showing p63 expression in different established melanoma cell lines. (D) P63 isoforms were overexpressed in MEL224 and LM1 cell lines. Empty vector was used as internal control. NTC stands for non-transfected cells. Cells harvested 48 hours' post-transfection for western blot analysis with p63, total and p-MEK1/2 antibodies. Similarly, A375M (E) cells infected with viral particles containing two different p63 shRNAs and pLKO.puro empty vector were harvested for western blot analysis after puromycin selection. (F) Enhancement of p-MEK1/2 expression upon transient expression of ΔNp63β isoform in A375M cells was abrogated by EGFR inhibitor (AG1478). Quantitative densitometry analysis of each protein band was normalized to GAPDH band. Average relative band intensity was calculated by Image Lab software from three independent experiments and plotted in reference to the first lane for each cell line for p-MEK1/2, total MEK1/2 and ΔNp63β protein expression. Error bars indicate standard error mean. *P < 0.05, **P < 0.01, ***P < 0.001, ns < non-significant.

Figure 2. Development and characterization of MAPKi resistant melanoma cell line. Established melanoma cell lines were chronically exposed to Vemurafenib or Trametinib for 8-12 weeks until the onset of a resistant phenotype. (A) Western blot analysis of WM793 cells compared with BRAFi resistant cells incubated with vehicle control DMSO (-), 3μM (+), or 6μM PLX4032 (++) for 24 hours. GAPDH was used as loading control. Densitometry analysis of each protein band was normalized to GAPDH band. Average relative band intensity was calculated by Image Lab software from three independent experiments and plotted in reference to the first lane for each cell line for p-MEK1/2 and total MEK1/2 protein expression. (B) and (C) *upper panel:* Western blot analysis of A375M (B) and WM164 (C) parental melanoma cell line and its respective chronically MEKi treated cell line were incubated with vehicle control DMSO (-) or 50nM Trametinib (+) for 24 hours. *Lower panel*: densitometry analysis of p-MEK1/2 and total MEK1/2 (B) and p-ERK1/2 and total ERK1/2 (C) protein expression normalized to GAPDH. (D) Equal number of BRAFi sensitive and resistant cells was seeded in 96-well plate and treated with increasing dose of PLX4032 in triplicates for 48 hours. After Alamar Blue staining, color change was measured with spectrophotometer. (E)

Growth curve of parental and MAPKi resistant melanoma cells over a period of 7-8 days. (F) FACS measurement of CD271 expression in MAPKi sensitive and resistant melanoma cell lines. The graph represents the average percentage of CD271 positive cells from three independent experiments. Error bars indicate standard error mean. *P < 0.05, **P < 0.01, ***P < 0.001, ns < non-significant.

Figure 3. Upregulated p63 expression contributes to development of MAPKi resistance in melanoma. (A) QRT-PCR analysis of p63 isoforms expression in different MAPKi sensitive and resistant melanoma cell lines. p63 transcript levels in NHEM (Normal Human Epidermal Melanocyte) are also shown. GUS was used as internal control. Average fold changes from three independent experiments were plotted in the graph. (B), (C), (D) Western Blotting analysis of p63 isoforms expression in (A) A375M, (B) LM36, LM16, LM17 cell lines before and after the acquisition of BRAFi resistance and (C) A375M and WM164 before and after the acquisition of MEKi resistance. The identity of isoforms was established by their co-migration with exogenously expressed p63 isoforms in HEK 293T cells. GAPDH was used as a loading control. Densitometry analysis of each protein band was normalized to GAPDH. (E) Western blot analysis of A375M cells stably expressing lentiviral particles containing empty vector and two different shRNA sequences targeting p63 isoforms. Average relative band intensity was calculated ΔNp63β protein expression. (F) Measurement of cell viability in A375M cells after p63 knockdown and treatment with 3μM PLX4032 (G) and in BRAFi resistant melanoma cells depleted from p63 exposed to increasing doses of PLX4032. After 48 hours treatment cells were stained with crystal violet and absorbance measured with spectrophotometer. Error bars indicate standard error mean. *P < 0.05, **P < 0.01, ***P < 0.001, ns < non-significant. (H) Immunofluorescence analysis of MART1 (red) and p63 (green) expression of clinical melanoma sample before combined treatment with MAPKi and after acquisition of MAPKi resistance. Images were taken on the INCell 2200 Analyser using 15% overlapped fields which were then stitched together using INCell Developer Toolbox. Scale bar = 100μm in the 2 panels and 40μm in the right enlargement, respectively.

Figure 4. Proteasomal degradation influences p63 stability in melanoma cells. (A) Western Blotting analysis of ΔNp63β expression in melanoma cell lines treated for 8 hours with proteasome inhibitor MG132 (2μM). GAPDH confirmed equal loading for all proteins. Western blot quantification is representative of three independent experiments. (B) QPCR analysis of specific FBXW7 isoforms (α, β and γ) in parental and MAPKi resistant melanoma cells. GUS was used as internal control. (C) and (D) Western blotting analysis of FBXW7 expression in parental and MAPKi resistant melanoma cell lines. GAPDH was used as loading control. Average band intensity is derived from three independent experiments. (E) Immunofluorescence analysis of FBXW7 expression and location in parental and BRAFi resistant melanoma cells. Cells were imaged using the automated INCell Analyser 6000 microscope. DAPI (blue) was used as nuclear counterstain and cell mask (grey) used as a whole cell dye. Scale bars represent 25μm. Experiments were performed in triplicates. (F) Nuclear (NER) and cytoplasmic (CYT) fractionation analysis of FBXW7 expression in parental and BRAFi resistant melanoma cells. GAPDH and Lamin A confirmed equal loading for cytoplasmic and nuclear fractions, respectively. Average band intensity from three independent experiments were plotted in the graph and normalized to the expression of GAPDH. (G) Immunoprecipitation analysis of p63 and FBXW7 endogenous interaction in WM1361 and A375M cells and (H) in Mel224 cells overexpressing specific p63 isoforms. (I) Western Blotting analysis of FBXW7 and ΔNp63β expression in A375M cells, upon ShRNA downregulation of FBXW7. GAPDH confirmed equal loading for all proteins. Average band intensity from three independent experiments were plotted in the graph and normalized to the expression of GAPDH. Error bars indicate standard error mean. *P < 0.05, **P < 0.01, ***P < 0.001, ns < non-significant.

Figure 5. Expression and location of mdm2 influence p63/FBXW7 interaction in MAPKi treated melanoma. (A) FBXW7 and MDM2 immunohistochemistry staining of melanoma clinical samples. Example of primary superficial spreading melanoma from trunk. Higher magnification images demonstrate nuclear FBXW7 and strong nuclear and cytoplasmic MDM2 reactivity. Black and white scales bar represent 200μm and 100μm distance, respectively. 31

for MDM2 and 24 for FBXW7 primary melanoma tumour nests were scored from 7 clinical samples based on the cytoplasmic and nuclear immunostaining intensity. Unpaired student t-test performed on mean expression values. ***P < 0.001. (B) QPCR analysis of MDM2 expression in parental and BRAFi resistant melanoma cells. (C) Western blotting analysis (left panel) and quantification (right panel) of MDM2 and MDM4 expression in parental and BRAFi resistant melanoma cells. (D) QPCR (left) and Western blotting analysis (right) of MDM2 expression in MEKi resistant melanoma cells. (E) Immunofluorescence analysis of MDM2 expression and location in parental and BRAFi resistant melanoma cells. Scale bar = 100µm. Experiments were performed in triplicates and average density levels (mean pixel value across the cell area) are displayed in the graph. (F) and (G) Nuclear (NER) and cytoplasmic (CYT) fractionation analysis of FBXW7 expression in parental and BRAFi (F) or MEKi (G) resistant cells. GAPDH and Lamin A confirmed equal loading for cytoplasmic and nuclear fractions, respectively. (H) Immunoprecipitation analysis of FBXW7 and MDM2 endogenous interaction in melanoma cell lines and HaCaT keratinocytes. (I) Western Blotting analysis of FBXW7 and ubiquitin upon in vitro ubiquitylation assay with mdm2. (J) Western Blotting analysis and quantification of FBXW7 expression in WM793 cells, upon overexpression with MDM2 plasmid with or without proteasome inhibitor MG-132. Densitometry analysis of each protein band was normalized to GAPDH. Average relative band intensity was calculated from three independent experiments. *P < 0.05, **P < 0.01, ***P < 0.001, ns < non-significant.

Figure 6. Nutlin-3A degrades p63 expression and sensitizes MAPKi resistant melanoma cells to apoptosis. (A), (B) Western Blotting analysis of p63 isoforms expression in WM793 parental (A) and BRAFi resistant (B) melanoma cells treated at increasing concentration of Nutlin-3A. Average band intensity from three independent experiments were plotted in the graph and normalized to the expression of GAPDH. (C) Western Blotting analysis of p63 expression in A375M cells Trametinib resistant treated at increasing concentration of Nutlin-3A. (D) QPCR analysis of p63 isoforms in WM793 cells treated with increasing concentration of Nutlin-3A. Relative fold change was calculated with reference to the internal control, GUS. (E) Analysis of FBXW7 expression in WM793 cells treated with increasing concentration of

Nutlin-3A by Western Blotting. (F) Western Blotting analysis of FBXW7 expression in WM278 parental as well as BRAFi resistant cells treated with 20μM Nutlin-3A. Average band intensity from three independent experiments were plotted in the graph and normalized to the expression of GAPDH. (G) QPCR analysis of FBXW7 isoforms expression in WM793 cells treated with 10μM Nutlin-3A. (H) Western Blotting analysis of FBXW7 expression in A375M cells after depletion of p53 and treatment with 10μM Nutlin-3A. (I) Western Blotting analysis of p63 isoforms expression in p53 mutated CHL-1 melanoma cells treated at increasing concentration of Nutlin-3A. (J) Measurement of apoptosis by FACS with Annexin V staining. Melanoma cell lines, treated for 24 hours with PLX4032 (3μM), Trametinib (50nM), Nut-3A (10μM), RG7112 (2.5μM), AMG232 (2.5μM) alone or combination. Graph represents the average percentage of total apoptotic cells from three independent experiments. Error bars indicate standard error mean. *P < 0.05, **P < 0.01, ***P < 0.001, ns < non-significant.

Figure 1

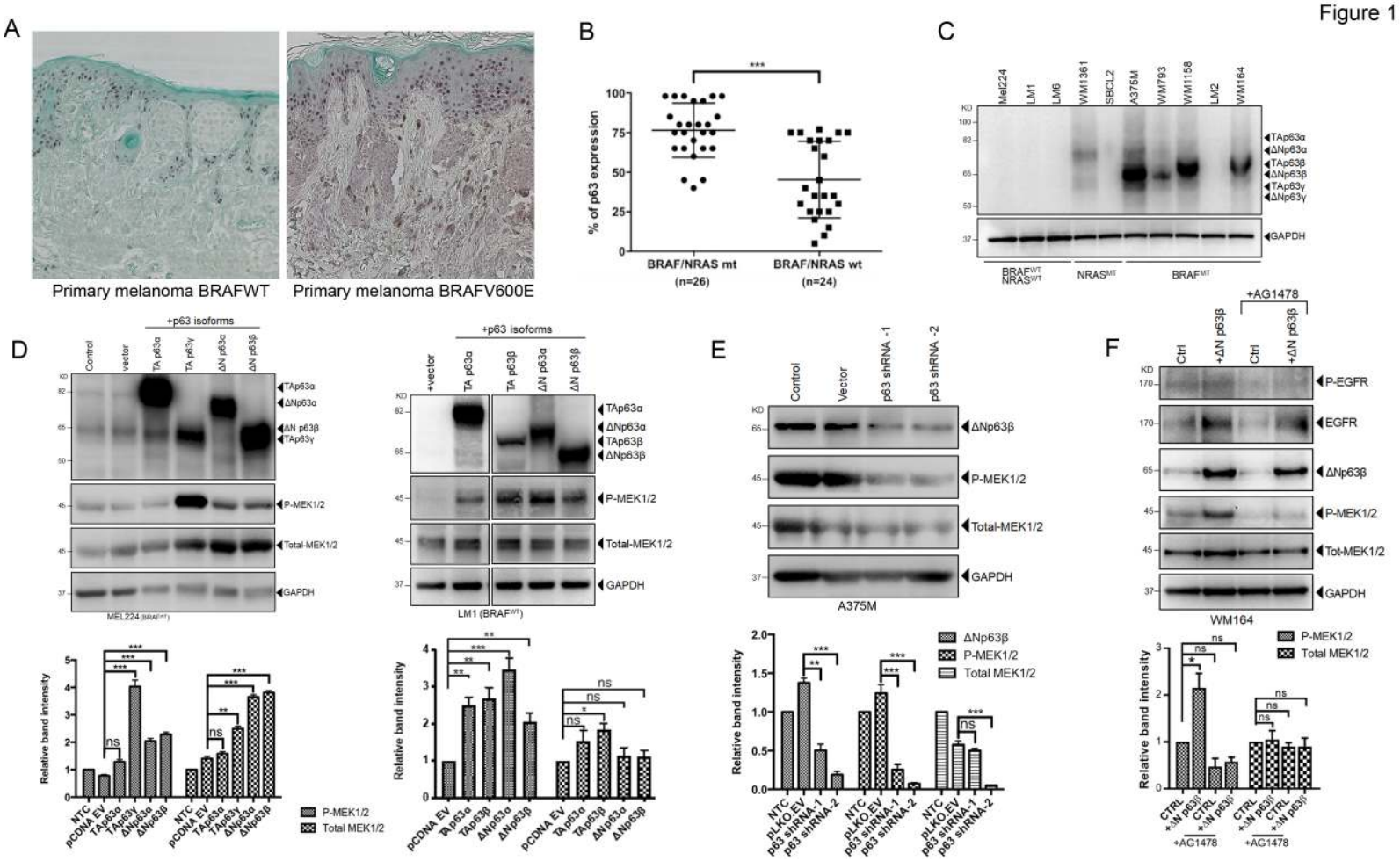
A
Primary melanoma BRAFWT
Primary melanoma BRAFV600E
B
% of p63 expression
BRAF/NRAS mt (n=26)
BRAF/NRAS wt (n=24)
C
Mel224
LM1
LM6
WM1361
SBCL2
A375M
WM793
WM1158
LM2
WM164
TAp63α
ΔNp63α
TAp63β
ΔNp63β
TAp63γ
ΔNp63γ
GAPDH
BRAFWT NRASWT
NRASMT
BRAFMT
D
+p63 isoforms
Control
vector
TA p63α
TA p63γ
ΔN p63α
ΔN p63β
ΔN p63γ
P-MEK1/2
Total-MEK1/2
MEL224 (BRAFMT)
+vector
TA p63α
TA p63β
ΔN p63α
ΔN p63β
LM1 (BRAFWT)
Relative band intensity
NTC
pCDNA EV
TAp63α
TAp63γ
ΔNp63α
ΔNp63β
TAp63β
E
Control
Vector
p63 shRNA -1
p63 shRNA -2
ΔNp63β
P-MEK1/2
Total-MEK1/2
GAPDH
A375M
pLKO.EV
p63 shRNA-1
p63 shRNA-2
F
+AG1478
Ctrl
+ΔN p63β
P-EGFR
EGFR
Tot-MEK1/2
WM164
CTRL
+ΔN p63β
+AG1478

Figure 2

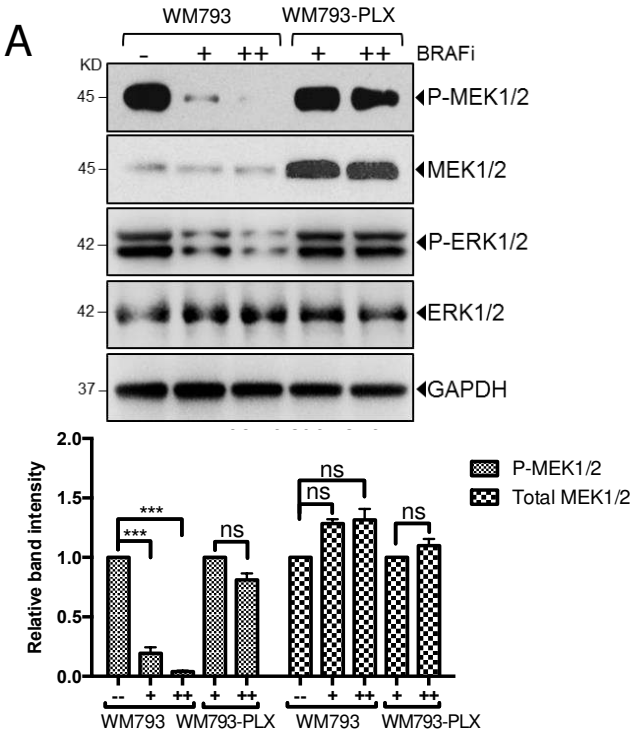
A
WM793
WM793-PLX
BRAFi
KD
P-MEK1/2
MEK1/2
P-ERK1/2
ERK1/2
GAPDH
Relative band intensity
P-MEK1/2
Total MEK1/2
ns
WM793
WM793-PLX

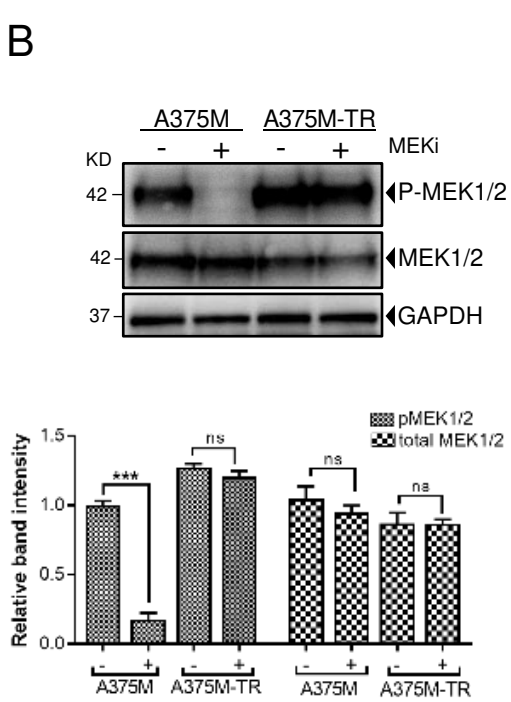
B
A375M
A375M-TR
MEKi
KD
P-MEK1/2
MEK1/2
GAPDH
pMEK1/2
total MEK1/2
Relative band intensity
ns

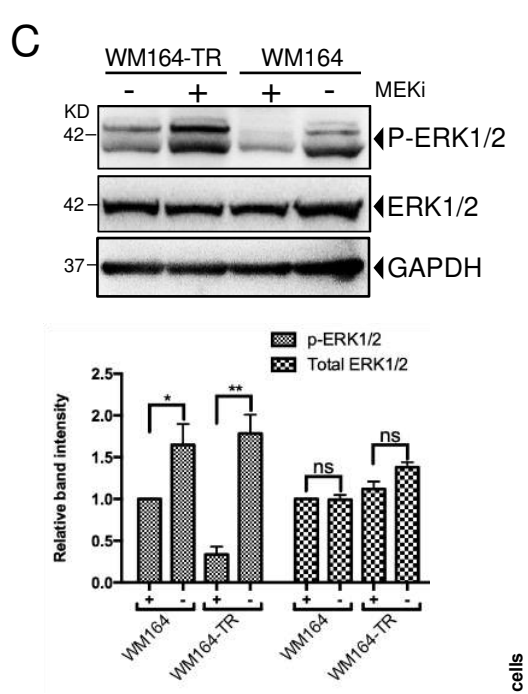
C
WM164-TR
WM164
MEKi
KD
P-ERK1/2
ERK1/2
GAPDH
p-ERK1/2
Total ERK1/2
Relative band intensity

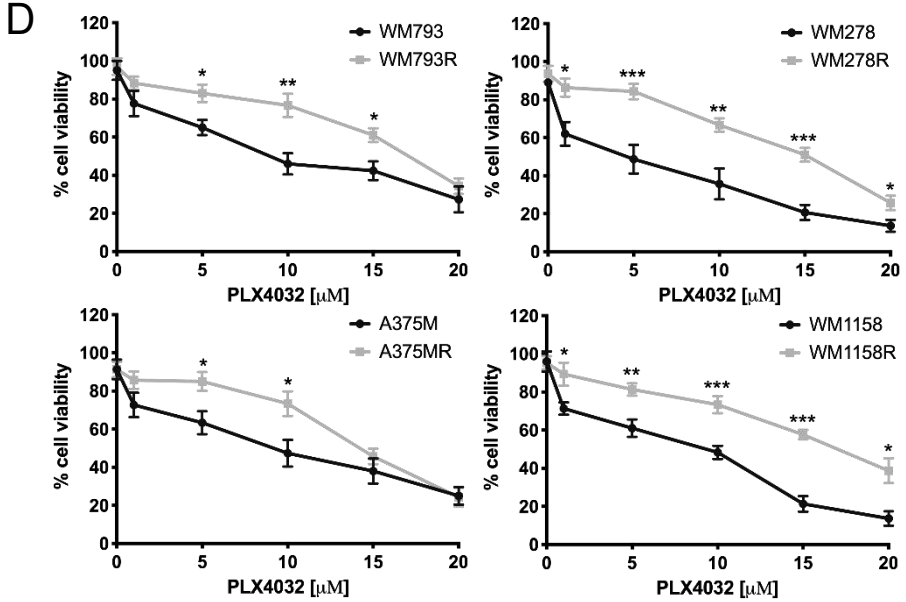
D
WM793
WM793R
WM278
WM278R
A375M
A375MR
WM1158
WM1158R
% cell viability
PLX4032 [μM]

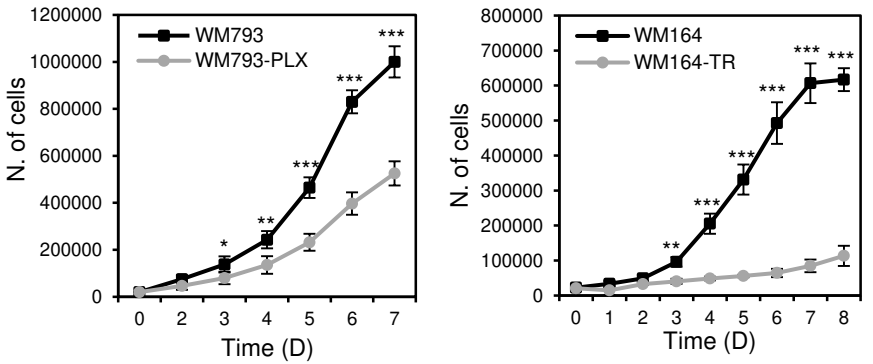
E
WM793
WM793-PLX
WM164
WM164-TR
N. of cells
Time (D)

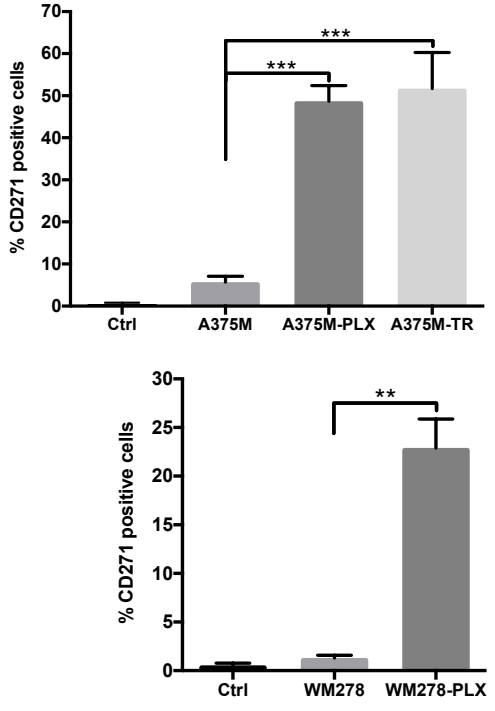
F
% CD271 positive cells
Ctrl
A375M
A375M-PLX
A375M-TR
WM278
WM278-PLX

Figure 3

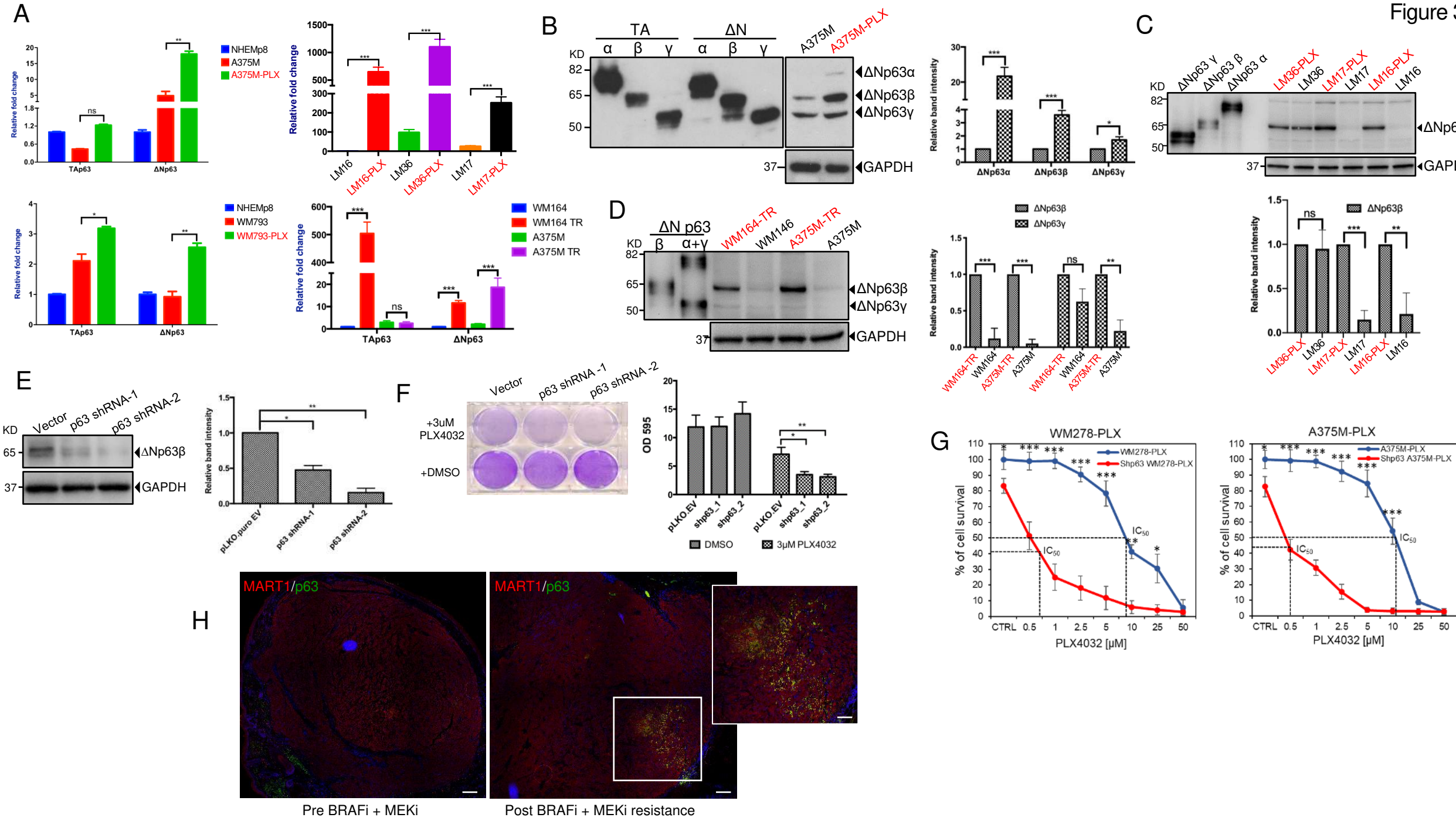
A
NHEMp8
A375M
A375M-PLX
Relative fold change
TAp63
ΔNp63
LM16
LM16-PLX
LM36
LM36-PLX
LM17
LM17-PLX
WM793
WM793-PLX
B
TA
ΔN
α β γ α β γ
KD
82
65
50
37
ΔNp63α
ΔNp63β
ΔNp63γ
GAPDH
Relative band intensity
C
ΔNp63 γ
ΔNp63 β
ΔNp63 α
D
ΔN p63
β α+γ
WM164-TR
WM146
A375M-TR
A375M
WM164
E
Vector
p63 shRNA-1
p63 shRNA-2
pLKO.puro EV
F
+3uM PLX4032
+DMSO
OD 595
pLKO.EV
shp63_1
shp63_2
DMSO
3μM PLX4032
G
WM278-PLX
Shp63 WM278-PLX
A375M-PLX
Shp63 A375M-PLX
% of cell survival
IC50
CTRL 0.5 1 2.5 5 10 25 50
PLX4032 [μM]
H
MART1/p63
Pre BRAFi + MEKi
Post BRAFi + MEKi resistance

Figure 4

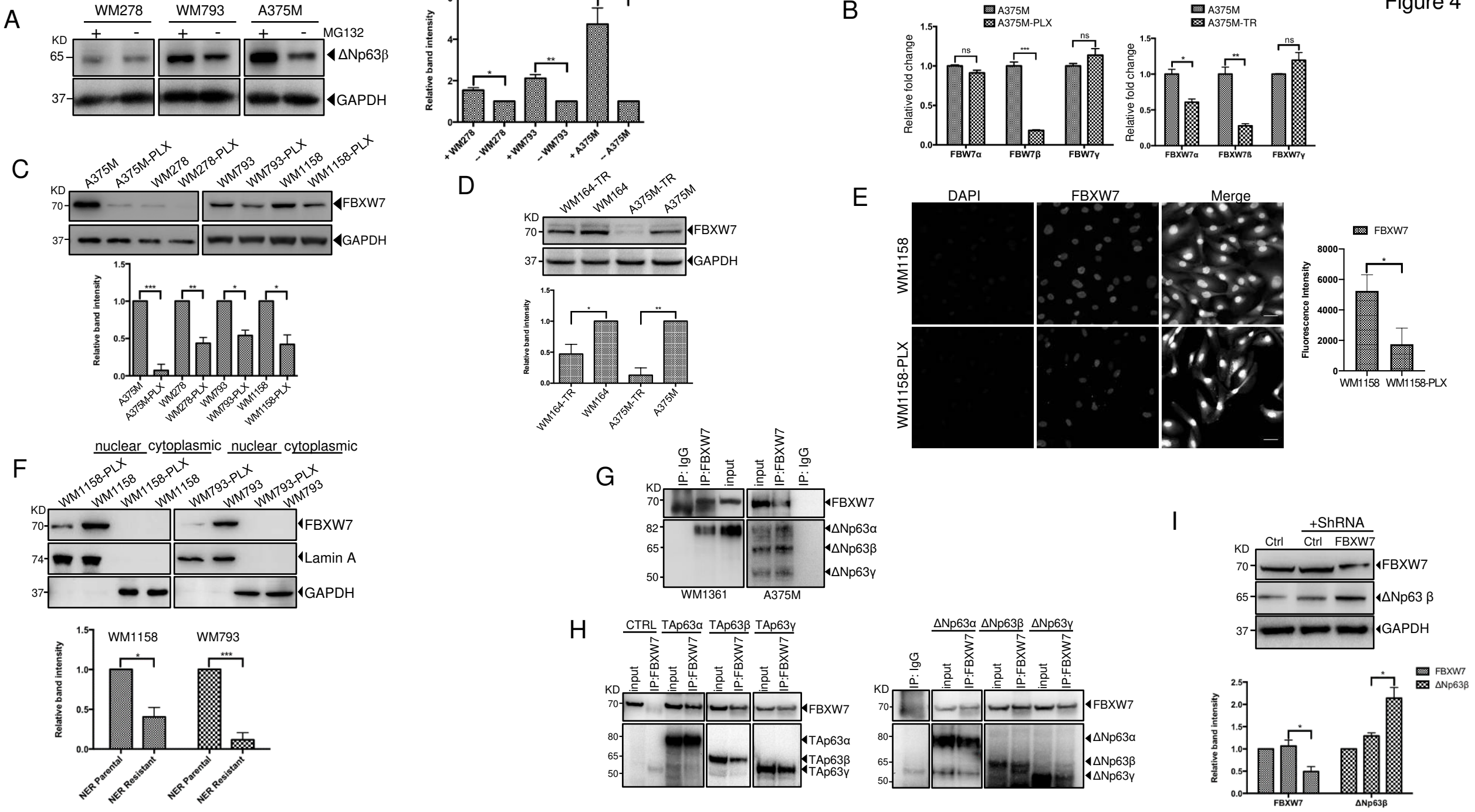
A
WM278
WM793
A375M
MG132
KD
65
37
ΔNp63β
GAPDH
Relative band intensity
+ WM278
- WM278
+ WM793
- WM793
+ A375M
- A375M
B
A375M
A375M-PLX
A375M-TR
Relative fold change
FBW7α
FBW7β
FBW7γ
FBXW7α
FBXW7ß
FBXW7γ
ns
C
A375M
A375M-PLX
WM278
WM278-PLX
WM793
WM793-PLX
WM1158
WM1158-PLX
FBXW7
GAPDH
D
WM164-TR
WM164
A375M-TR
A375M
E
DAPI
FBXW7
Merge
WM1158
WM1158-PLX
Fluorescence Intensity
F
nuclear
cytoplasmic
Lamin A
NER Parental
NER Resistant
G
IP: IgG
IP:FBXW7
input
ΔNp63α
ΔNp63β
ΔNp63γ
WM1361
A375M
H
CTRL
TAp63α
TAp63β
TAp63γ
TAp63α
TAp63β
TAp63γ
I
+ShRNA
Ctrl
FBXW7
ΔNp63 β

Figure 5

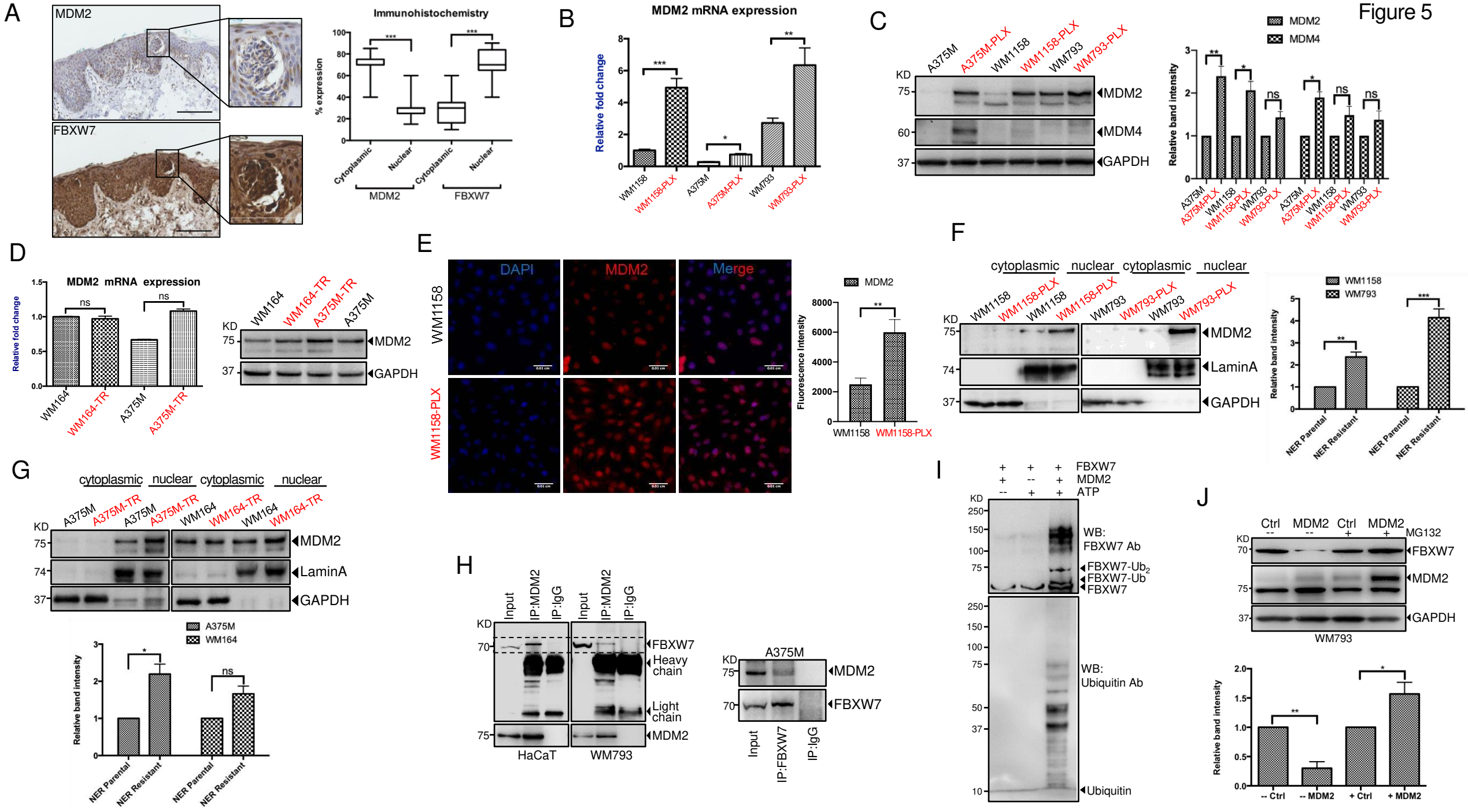
A
MDM2
FBXW7
Immunohistochemistry
% expression
Cytoplasmic
Nuclear
MDM2
FBXW7
B
MDM2 mRNA expression
Relative fold change
WM1158
WM1158-PLX
A375M
A375M-PLX
WM793
WM793-PLX
C
KD
MDM2
MDM4
GAPDH
Relative band intensity
D
MDM2 mRNA expression
WM164
WM164-TR
A375M-TR
E
DAPI
MDM2
Merge
Fluorescence Intensity
F
cytoplasmic
nuclear
LaminA
NER Parental
NER Resistant
G
H
Input
IP:MDM2
IP:IgG
Heavy chain
Light chain
HaCaT
IP:FBXW7
I
FBXW7
MDM2
ATP
WB:
FBXW7 Ab
FBXW7-Ub2
FBXW7-Ub
WB:
Ubiquitin Ab
Ubiquitin
J
Ctrl
MG132
-- Ctrl
-- MDM2
+ Ctrl
+ MDM2

Figure 6

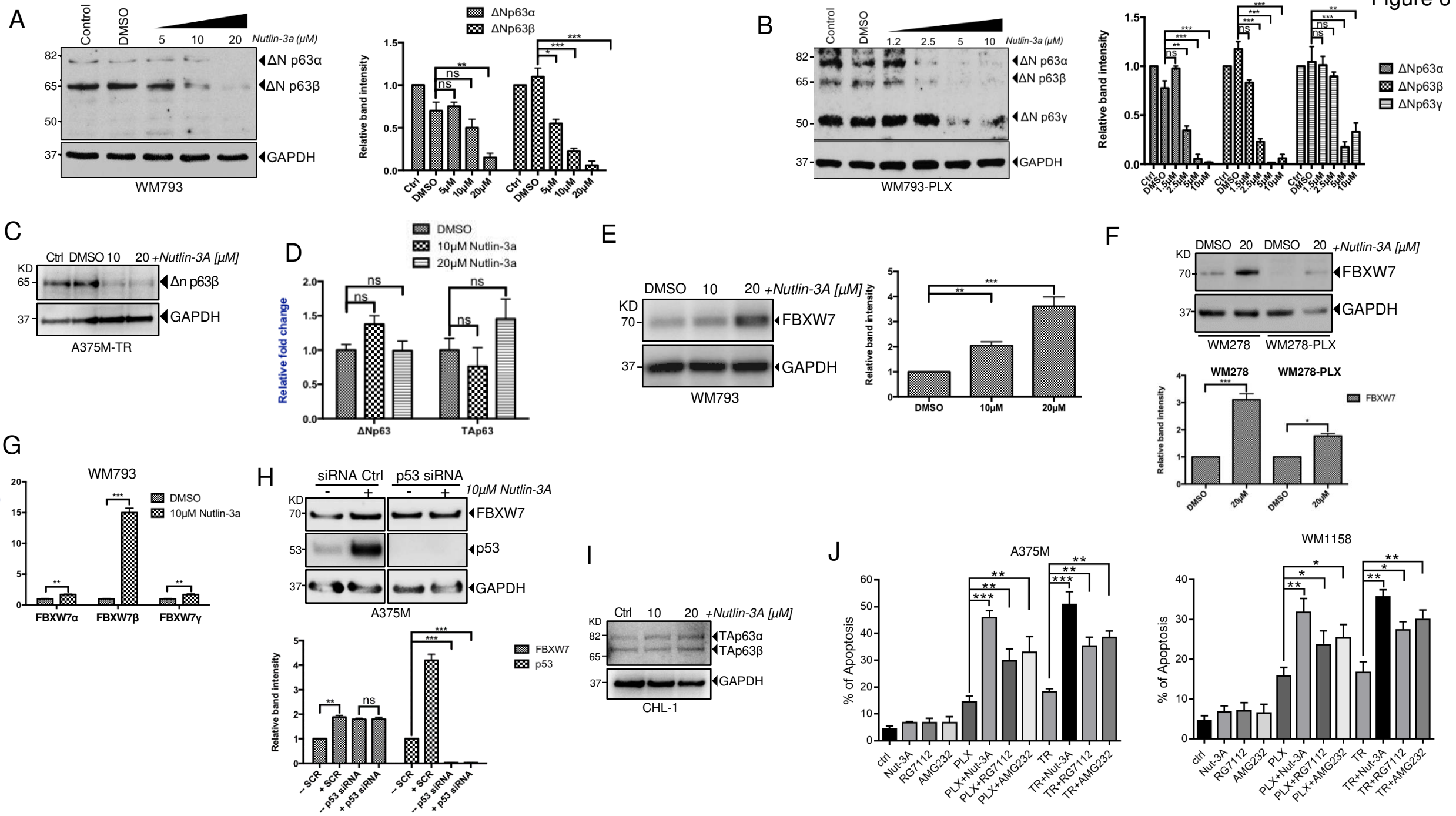
A
Control
DMSO
5
10
20
Nutlin-3a (μM)
82
65
50
37
ΔN p63α
ΔN p63β
GAPDH
WM793
ΔNp63α
ΔNp63β
Relative band intensity
Ctrl
DMSO
5μM
10μM
20μM
B
1.2
2.5
ΔN p63γ
WM793-PLX
ΔNp63γ
C
Ctrl DMSO 10 20 +Nutlin-3A [μM]
KD
Δn p63β
A375M-TR
D
DMSO
10μM Nutlin-3a
20μM Nutlin-3a
Relative fold change
ΔNp63
TAp63
E
FBXW7
WM793
F
WM278
WM278-PLX
G
WM793
FBXW7α
FBXW7β
FBXW7γ
H
siRNA Ctrl
p53 siRNA
10μM Nutlin-3A
p53
A375M
-- SCR
+ SCR
-- p53 siRNA
+ p53 siRNA
I
TAp63α
TAp63β
CHL-1
J
A375M
WM1158
% of Apoptosis
ctrl
Nut-3A
RG7112
AMG232
PLX
PLX+Nut-3A
PLX+RG7112
PLX+AMG232
TR
TR+Nut-3A
TR+RG7112
TR+AMG232